

Application of the Normalized Difference Vegetation Index with Satellite Imagery in Warints-Yawi Communities

Miguel Angel Osorio Rivera¹

miguel.osorio@epoch.edu.ec (<https://orcid.org/0000-0002-8641-2721>)

Juan Pablo Haro Altamirano²

juanpablo.haro@epoch.edu.ec (<https://orcid.org/0000-0001-8538-3191>)

Sandra Elizabeth López Sampedro³

salopez@epoch.edu.ec(<https://orcid.org/0000-0003-0209-2087>)

William Estuardo Carrillo Barahona⁴

estuardo.carrillo@epoch.edu.ec (<https://orcid.org/0000-0002-1432-9638>)

Justo Moises Narvaez Brito⁵

moises4271@gmail.com (<https://orcid.org/0000-0001-7583-9423>)

Escuela Superior Politécnica de Chimborazo^{1,2,3,4}; Investigador Independiente⁵

Article Info

Page Number: 759 - 772

Publication Issue:

Vol 72 No. 1 (2023)

Article History

Article Received: 15 October 2022

Revised: 24 November 2022

Accepted: 18 December 2022

Abstract

The purpose of the study was to analyze the behavior of the normalized difference vegetation index of the communities of Warints and Yawi, located in the Limón Indanza canton, province of Morona Santiago, during the summer season. The methodology is descriptive, non-experimental and longitudinal, with 13 samples taken from June to September, from 1998 to 2022, taken from LandSat 5 and 8 of the TM and OLI sensors, respectively, with a cloud cover of 30%, the radiometric and atmospheric calibration was established and the NDVI was determined with ENVI 5.3. It was mapped in ArcGis 10.5, extracting the data for the application of statistical analysis (t Student at 5%). The average NDVI was 0.66, with maximum and minimum values of 0.925 and -0.033, respectively; with a negative trend line. It was concluded that a large part of the study area corresponds to native forest; however, the negative trend is due to anthropogenic activities and territorial growth of the communities. It is recommended to apply this study approach to explore and apply in similar areas.

Keywords: << Landsat, NDVI, Remote sensing, Amazonia, Vegetation >>

I. INTRODUCTION

Information on vegetation is essential to understand changes in the ecosystem process and its associated impacts over time (1), such as phenomena related to biodiversity loss, desertification, relationship between vegetation and soil erosion (2); being considered in cities an important

component for urban ecosystems, contributes to a wide range of functions in ambient quality (3), where the higher the percentage of vegetation cover the greater the ecological benefits, thus reducing heat islands (4) and in turn air pollution; All these aspects relate to the risk and well-being of human health.

Currently, technological tools have been developed that allow the acquisition of spatial information of this type, without having direct contact with the phenomena (5), it is Remote sensing used as a complement to studies oriented to the environment (6), supported by geographic information systems (GIS) to concentrate the data generated (Maldonado et al. 2015).

Vegetation indices are derived techniques, in which they take advantage of the particular radiometric behavior of healthy vegetation in the different spectral bands, especially between visible and near-infrared (8). One of them is the differential normalized index of vegetation (NDVI) according to Campos (et al. 2018) This index yields estimated values of forest greenness resulting from the analysis of satellite data; according to Ren (et al. 2017), it is the most widely used spectral indicator where most Land sat satellite images are used with TM and/or OLI sensors. , they are easily accessible worldwide to extract and estimate the structural attributes of vegetation.

During the last decades, there were many studies focused on spatiotemporal changes in vegetation (10); Miller (2012) conducted research regarding urban vegetation, focusing on changing the percentage of vegetation cover, which showed open green spaces in Changchun City, China in 2010 reached 45% of the total area.

The indicator also discriminates against agricultural crops, in the study by Mirasi et al. (2021) estimates wheat grain yield using multi-temporal OLI Landsat data; It concluded that the NDVI sum values were more accurate than the estimate by adding the four applied vegetation index values, also for Singlasugarcane (et al. 2018) indicated the best period for sugarcane crop discrimination in the Himalayan foothills region, using Landsat 8 satellite imagery for monitoring and discrimination.

In Ecuador, studies were carried out in relation to the decrease in vegetation cover used in Landsat multispectral images of 1998, 2008 and 2018; the average NDVI was 0.549; 0.254 and 0.479, respectively, what was noticed was that between 1998-2008 a negative trend was observed, which evidenced a decrease in vegetation cover of 498.47 km² (64%) (14). On the other hand, research was given to determine the vegetation cover and land uses in Manabí, Ríos (et al. 2016) concluded that the classification of the NDVI values coincides with the main types of vegetation cover and land uses present in the study areas, with a reliability percentage between 80 and 90%.

The objective of the research was to analyze the behavior of the normalized difference vegetation index in the communities of Warints and Yawi, in summer times, being from June to September, from the year 1998 to the year 2022.

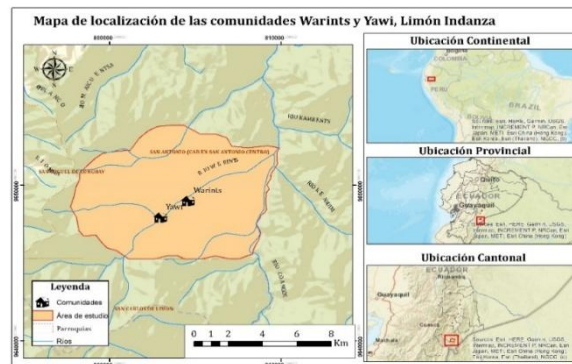
II. MATERIALS AND METHODS

The methodology used is descriptive, non-experimental, longitudinal contrast. It is divided into three main stages: description of the study area, data and processing of images, calculation of indices, and these are detailed below.

AREA OF STUDY

The study area is located in the communities of Warints and Yawi, located in the Palora canton, province of Morona Santiago, is at geographical coordinates $3^{\circ} 4'23.98''\text{S}$ and $78^{\circ} 20'19.35''\text{W}$, has an altitude of between 1,000 to 1,400 m. s.n.m., its climate is temperate and humid, maintains an average temperature of 18°C to 22°C . The average rainfall ranges from 1500 mm to 3000 mm (16). For the study, a specific area was delimited with an extension of 79,578 km² that encompasses both communities, the commune limits were established due to the lack of proportionality of current vector information of the area.

Figure 1. Location map of the Warints and Yawi communities, Limón Indanza.



DATA ACQUISITION

The satellite images were obtained according to the territory or the geographical area under study, on November 20, 2022 from the database of the Landsat satellites of the United States Geological Survey (USGS) (<https://earthexplorer.usgs.gov/>) sensors used: Landsat 5 TM and Landsat 8 OLI (**figure 2**), with a UTM (Universal Transverse Mercator) projection, zone 17 S with path: 009, row: 069 for the months June to September, from 1998 to year 2022 (**Table 1**); the information is in Geo TIFF format with a spatial resolution of 30x 30m with a cloud coverage of 5%.

Table 1. Data from the Landsat images used for the determination of the NDVI in the period 1998-2022.

No.	Date	Sensor
1	1998-09-25	Landsat 5 TM
2	1999-07-10	Landsat 5 TM
3	2000-08-29	Landsat 5 TM
4	2003-10-25	Landsat 5 TM
5	2006-09-15	Landsat 5 TM
6	2007-09-18	Landsat 5 TM

7	2011-08-12	Landsat 5 TM
8	2015-08-07	Landsat 5 TM
9	2016-09-14	Landsat 8 OLI
10	2018-07-18	Landsat 8 OLI
11	2019-08-18	Landsat 8 OLI
12	2020-08-04	Landsat 8 OLI
13	2022-08-10	Landsat 8 OLI

PREPROCESAMIENTO

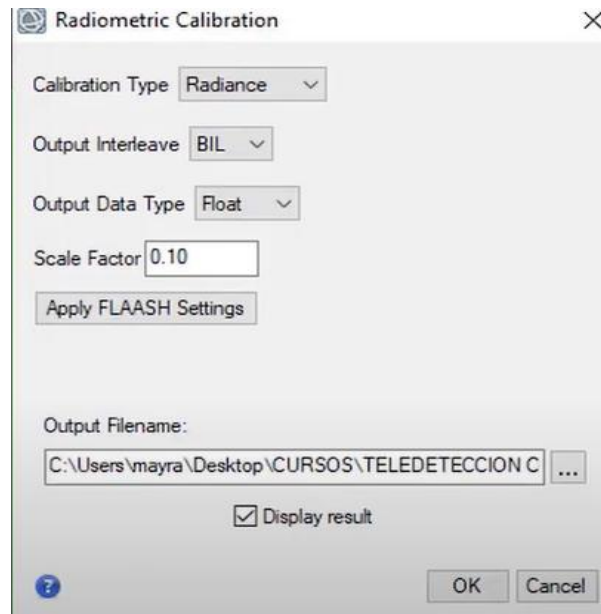
The coverage area of the Landsat images present a greater surface area in relation to the area under study, therefore, it is necessary to make a crop in order to obtain the delimitation of the work area (17); in this process to delimit the area of interest the map of Administrative Political Vision of Ecuador was used. obtained from the IGM (Military Geographic Institute). From this map, and using the ENVI 5.3 software, through the Subset Data from ROIs tool, the mosaic was cropped.

Prior processing of the data in question is necessary before starting any analysis of the information collected from a remote sensor (18). For this, two types of pre-processing are carried out: radiometric and atmospheric correction, the latter compensating for the effects of environmental factors and problems of sensor malfunction (Ambrosio et al. 2012), instead the atmospheric Brizuela (et al. 2007) It mentions that it helps eliminate the effect of aerosols, dispersion of molecules, particles and intrinsic radiance that is introduced into the sensor and is reflected in the image.

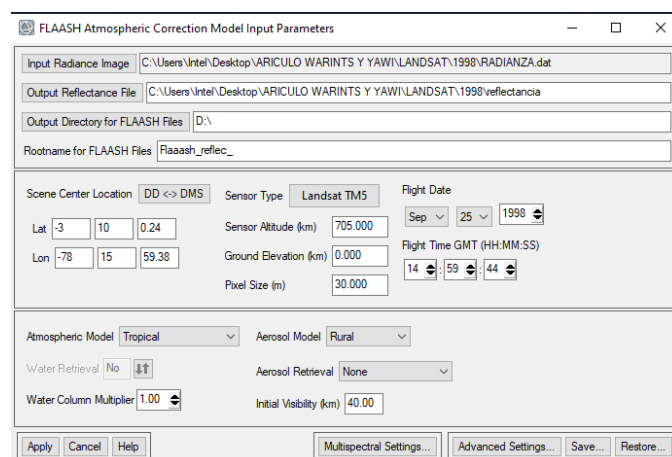
The study used the use of the ENVI 5.3 application, from the file containing the extension _MTI.txt, which corresponds to the image format with metadata available for Landsat this opens from the option of File/Open as/Landsat/GeoTIFF with Metadata; the methodology exposed by Aguilar (et al. 2015), radiometric correction is first performed using the Radiometric Calibration tool (Toolbox/Radiometric Correction/ Radiometric Calibration); First, the image is divided into 5 segments in which include the multispectral bands (which has the infrared), the Cirrus band, thermal, panchromatic and quality; from these the MultiSpectral must be selected and assign the different calibration values present in Table 2 and expressed in Figure 2.

Table 2. Radiometric calibration values for Landsat 5 and 8 (22).

Field	Value
Type of calibration	Radiancia
Output interval	WAS
Output data type	Floating
Scale factor	0.10
Output directory	Output name and directory

Figure 2. Empleo of the values for radiometric calibration in the Radiometric Calibration tool.

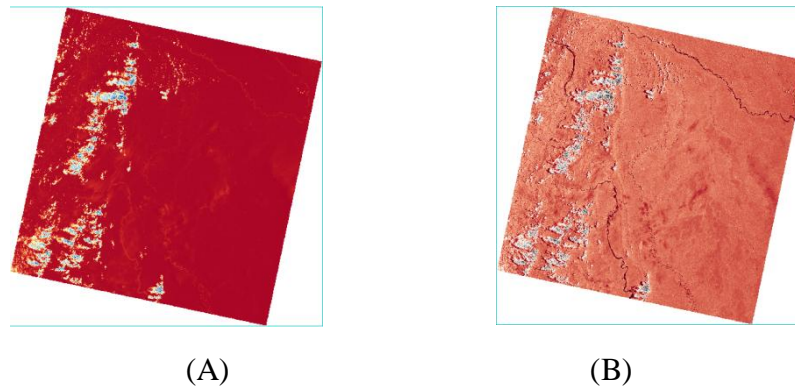
At the end of the process, an image is obtained with digital values corresponding to radiance in BIL metadata format. From this file the atmospheric correction is made using the FLAASH tool; the required parameters are: leave the option unknown-MSI (UNKNOWN-MSI), at the altitude of the sensor: 705 km and the pixel size is automatically placed, as well as the values of Lat-Long; the elevation will vary for each image, in addition to the date and time of flight (extract from the metadata); Values used in Figure 3.

Figure 3. Use of values for atmospheric calibration in the FLAASH tool tool.

At the end of the treatment of the images, an orthophoto is generated

CONSTRUCTION OF THE NDVI TIME SERIES

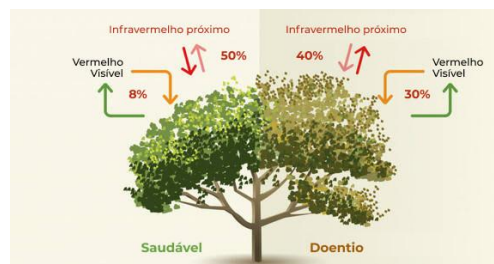
NDVI is based on the differences in reflectivity between red and near-infrared (23) both of which are shown in Figure 4.

Figure 4. Red and infrared spectra of study areas

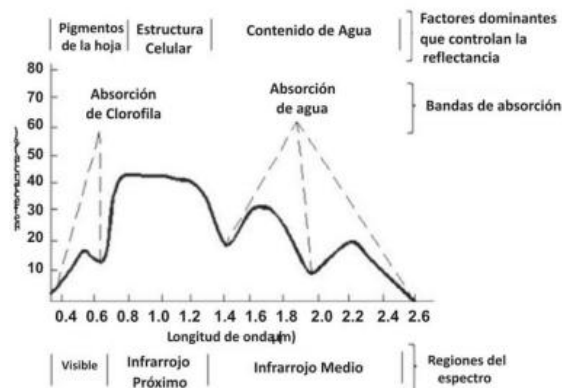
Note: (A) Red spectrum; (B) Infrared spectrum (24).

Tovar (2011) uses it through the relationship between the energy absorbed and emitted by the vegetation covers, thus allowing to determine through the values of radiation that emits or reflects the intensity of the greenery of the area, the amount of vegetation, state of health of the plants, evolution and plant vigor.

Chlorophyll is able to absorb most visible red light, in addition to strongly reflecting near-infrared light. Therefore, dense vegetation will have lower reflectance in the red and near-infrared band as depicted in Figure 5 and 6.

Figure 5. Absorption of red and infrared spectra in the plant

Note: NDVI representation based on satellite imagery used (26).

Figure 6. Standard curve of plant reflectance .

Note: Representation of the reflectance of a plant structure at different wavelengths (Visible, Infrared and Mid-Infrared) (27).

NDVI is calculated from visible red and near-infrared reflectance measurements in the region of the electromagnetic spectrum (28). Se deduces with the following formula:

$$NDVI = \frac{(Infrarrojo) - (Rojo)}{(Infrarrojo) + (Rojo)} \quad (1)$$

The USGS (2016) states that the NDVI of TM and ETM+ sensor images is calculated from bands 3 and 4. It is expressed as follows:

$$NDVI_{TM-ETM+} = \frac{(B4) - (B3)}{(B4) + (B3)} \quad (2)$$

Where B4 and B3 are the reflectances in the near-infrared and visible bands, respectively.

On the other hand, for the OLI sensor, the NDVI is calculated from bands 4 and 5 (29). It states as follows:

$$NDVI_{TM-ETM+} = \frac{(B5) - (B4)}{(B5) + (B4)} \quad (2)$$

Where B5 and B4 are the reflectances in the near-infrared and visible bands, respectively.

The NDVI is a dimensionless index and can take values between -1, 0 and 1.0, where negative values (-1) to zero (0) are discovered areas, while (0) to (1) indicate the presence of plants; In an approximate range of (0.5) and (0.7) there is the presence of dense vegetation (30).

In the study by Mejía et al. (2021), NDVI is used to categorize land use in the northern Amazon of Ecuador, establishing the following categories (Table 3):

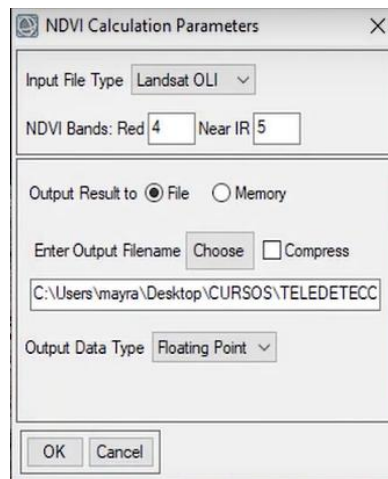
Table 3. NDVI Categories

Type of vegetation	Rank
Soil without vegetation, water, shadows	<0,2
Soil withp oca vegetation	0,2-0.44
Sparse vegetation	0,45-0,55
Scattered vegetation	0,56-0,65
Forest	>0,65

Note: Each category represents a different characteristic for Soil without vegetation, water, shadows: Much of the soil corresponds to dark areas and linked to rivers, Soil with little vegetation: Coincides with urban areas, Sparse vegetation: Soils in process of transformation and grasslands, Dispersed vegetation: Soils linked to agricultural activity, shrub and herbaceous vegetation, Forest: Soil with abundant shrub vegetation (Mejía et al. 2021).

The NDVI time series was elaborated from the 15 satellite images, using the NDVI tool of the ENVI software (Toolbox/Spectral/ Vegetation/ NDVI) in order to monitor plant vigor (Figure 7).

Figure 7. Use of the NDVI Calculation Parameters tool in ENVI 5.3.



Note: It will depend on the type of satellite (ENVI 5.3, 2022).

Statistical analysis

For statistical analysis, the data obtained from the ENVI 5.3 software in ArcGis 10.5 were processed using the Excel 2019 application. Likewise, the statistical technique of comparing means through Student's t-test was used for a sample with a significance level of 0.05 (5%).

III. RESULTS

As a result of the analysis of the maps and the raster, the statistical values of the NDVI from 1998 to 2022 were obtained (table 4), it was obtained that the minimum NDVI value was -0.033 which corresponds to the Warints River and cloud cover; with a maximum value of 0.925 which belongs to native forest areas. The average NDVI from 1998 to 2022 was 0.546, which represents 0.66 corresponding to soil with abundant shrub vegetation.

Table 4: NDVI statistical values of the study area from 1998 to 2022

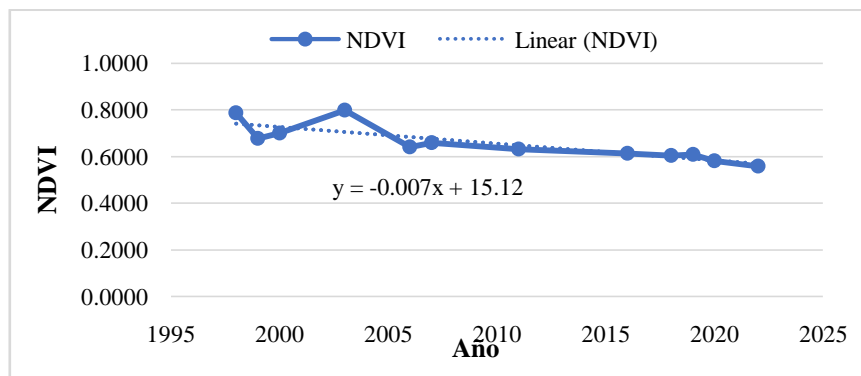
Year	V _{mín}	V _{max}	μ NDVI	S
1998	-0,065	0,925	0,788	0,090
1999	-0,098	0,775	0,678	0,101
2000	-0,072	0,771	0,699	0,066

2003	-0,223	0,751	0,799	0,139
2006	-0,060	0,757	0,640	0,093
2007	-0,046	0,740	0,658	0,072
2011	0,094	0,762	0,632	0,047
2016	0,046	0,596	0,613	0,069
2018	0,026	0,619	0,605	0,134
2019	0,022	0,583	0,609	0,090
2020	-0,033	0,599	0,582	0,058
2022	0,016	0,605	0,559	0,096

Note: V_{mín}: Minimum values, V_{máx}: Maximum values, μ NDVI: Average NDVI and σ : Standard deviation.

Figure 8 represents the trend line presented with the NDVI values as a function of annuities, it is observed that there is a negative trend, which means a considerable decrease in vegetation at different times.

Figure 8. NDVI average based on annual periods and trend line.



In the test of distribution t of Student for a factor, the null hypotheses were established in relation to the normalized difference vegetation index of the Warints and Yawi communities from 1998 to 2022; if the index is greater than 0.2 and less than 0.23. For the first hypothesis, Table 2 shows that the experimental t is greater than the critical; added to this, the p -value that is less than the significance (0.05), which means that the null hypothesis is accepted, the NDVI being greater than or equal 0.23.

Table 2: Values obtained from t Student

t experimental	19,519
theoretical t	2,201
Degrees of freedom	11
p-value	3,4x10-10

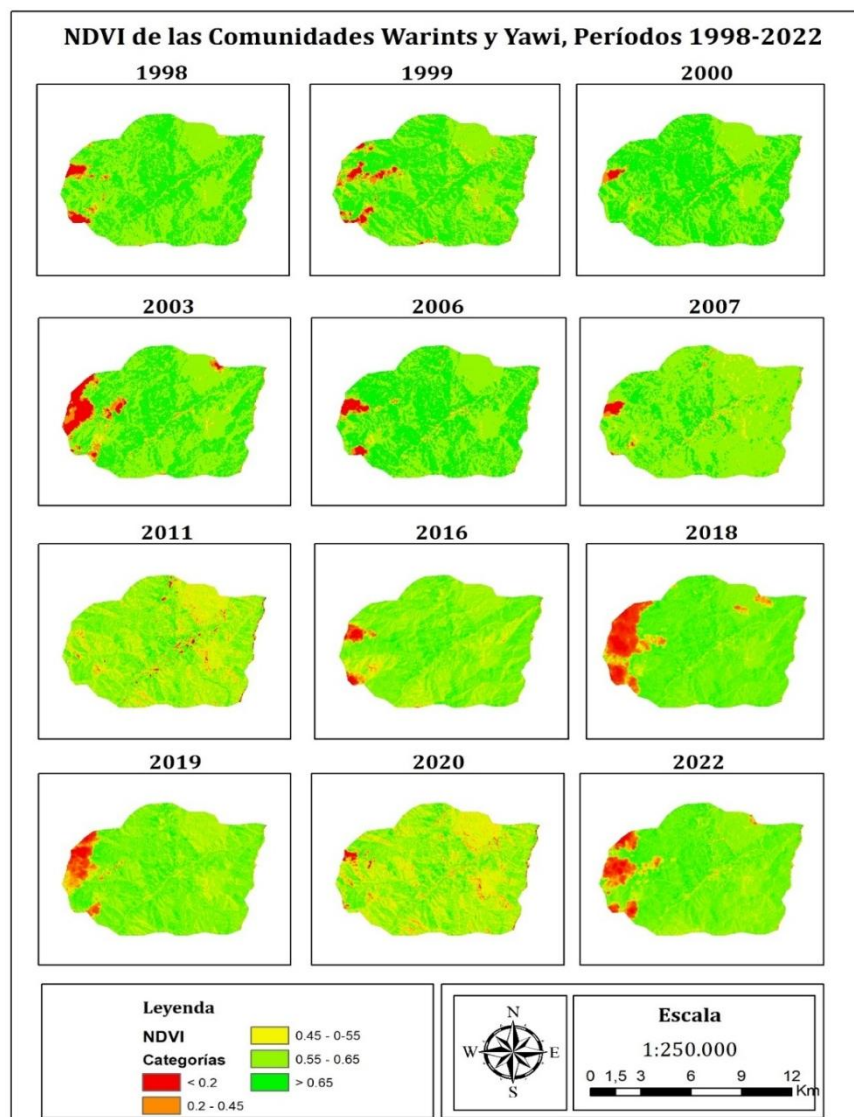
The second assumption of the null hypothesis, if the NDVI index is less than or equal to 0.20; established in table x, results in the hypothesis being rejected because the p-value is greater than the significance (0.05).

Table 2: Values obtained from t Student

t experimental	20,896
theoretical t	2,201
Degrees of freedom	11
p-value	1

In Figure 9. the various changes in the NDVI index over the years represented by maps are observed for a better understanding of the results obtained from the Warints and Yawi communities.

Figure 9. Maps of the study area with NDVI representation based on 1998-2022 annuities



IV. DISCUSSION

In the present study, the evaluation of the categorization of the Normalized Difference Vegetation Index showed a high vegetative contribution of 0.66, corroborating these data at the provincial level due to the lack of local studies; the results are related to the study conducted by Chamba (2015) (32). on the spatial temporal dynamics of the EVI vegetation index in the southern part of Ecuador, where it concluded that Morona Santiago obtained an average value of 0.53 characterized as native forest with high vegetative density, likewise the answers given in the research used in soils of the northern Amazon of Ecuador in the period 2012-2019 by Mejía et al. (2021) obtain values of 0.54, 0.64 and 0.7 for Nueva Loja, Shushufindi and La Joya de los Sachas, respectively, meaning that native forest largely prevails.

The distribution of the area maintains a negative trend level of the index, which is due according to Maldonado et al. (2015), (7) to factors such as illegal mining, timber extraction or overgrazing. In turn, Zou et al. (2022) (1) assume that vegetation growth conditions are related to climatic and vegetation characteristics. This decrease also leads to deduce that the changes are due to the anthropic activities of the area and the population growth of the communities, which has caused a continuous process of transformation of the territory. In the research, a sudden change was noted in the central areas of the communities, which coincides with Aldás (2019), (33) research used in the Cotacachi Cayapas Ecological Reserve clearly appreciates anthropic processes in ranges of 0.55 during annual changes. In addition, it was possible to appreciate negative values of the index this is due to the bodies of water within the images, which corroborates with Brito et al. (2021) (34), applied the NDVI for the extraction of the Upano river basin for further analysis.

V. CONCLUSIONS

The behavior of the normalized difference vegetation index in the communities of Warints and Yawi, in summer times (June to September), from 1998 to 2022 was analyzed; the results showed that the vegetation index of the study area 0.66 being largely native forest, also presented a negative trend to depending on the years this is due to anthropogenic activities and territorial growth of the communities.

The study mapped the NDVI change combined with Landsat 5 and 8 images, going so far as to demonstrate that they can provide a fast and cost-effective method to obtain a 30m resolution structural dataset of vegetation. The proposed approach can also be explored and applied in other similar areas.

VI. CONFLICT OF INTEREST

There is no conflict of interest or problems in publishing the data obtained in this study.

VII. REFERENCES

1. Zou D, Zhao L, Liu G, Du E, Hu G, Li Z, et al. Vegetation Mapping in the Permafrost Region: A Case Study on the Central Qinghai-Tibet Plateau. Remote Sensing [Internet]. 5 de enero de

- 2022 [citado 4 de octubre de 2022];14(1):232. Disponible en: <https://www.mdpi.com/2072-4292/14/1/232>
2. Gonzaga C. Application of vegetation indices derived from satellite images for analysis of vegetation cover in the province of Loja, Ecuador. CEDAMAZ [Internet]. 2015 [cited 11 September 2022];5(1):30-41. Available in: <https://revistas.unl.edu.ec/index.php/cedamaz/article/view/43>
 3. Ren Z, Pu R, Zheng H, Zhang D, He X. Spatiotemporal analyses of urban vegetation structural attributes using multitemporal Landsat TM data and field measurements. *Annals of Forest Science* [Internet]. septiembre de 2017 [citado 19 de noviembre de 2022];74(3):1-14. Disponible en: <https://annforsci.biomedcentral.com/articles/10.1007/s13595-017-0654-x>
 4. Iizuka K, Tateishi R. Estimation of CO₂ Sequestration by the Forests in Japan by Discriminating Precise Tree Age Category using Remote Sensing Techniques. *Remote Sensing* [Internet]. noviembre de 2015 [citado 19 de noviembre de 2022];7(11):15082-113. Disponible en: <https://www.mdpi.com/2072-4292/7/11/15082>
 5. Chuvieco E. Fundamentals of spatial remote sensing. 2nd ed. Spain: Rialp; 1995.
 6. Fernández I, Herrero E. Visual Analysis of Images Obtained from the ETM+ Sensor-Landsat Satellite [Internet]. University of VALLADOLID. 2001 [cited 7 August 2022]. Available in: <https://fdocuments.ec/document/analisis-visual-de-landsat.html>
 7. Maldonado J, Alatorre L, Torres M. Analysis of NDVI Trends with Satellite Imagery in Cuauhtémoc, Chihuahua (2000-2014). 2015;6. Available in: <https://www.uacj.mx/CGTI/CDTE/JPM/Documents/SELPER/assets/m017.pdf>
 8. Chuvieco E. Environmental remote sensing. The observation of the earth from space [Internet]. 3rd ed. Barcela; 2008. 592 p. Available in: <https://tysmagazine.com/libro-gratuito-teledeteccion-ambiental-la-observacion-la-tierra-desde-espacio/>
 9. Campos A, Guerrero E, Gines E. Evolution of vegetation cover in the Cerros de Amotape de Tumbes National Park using the Normalized Difference Vegetation Index (NDVI): 2000 – 2014. *Mangrove* [Internet]. 2018 [cited 19 November 2022];15(1):47-56. Available in: <https://erp.untumbes.edu.pe/revistas/index.php/manglar/article/view/92>
 10. Seto KC, Woodcock CE, Song C, Huang X, Lu J, Kaufmann RK. Monitoring land-use change in the Pearl River Delta using Landsat TM. *International Journal of Remote Sensing* [Internet]. 1 de enero de 2002 [citado 19 de noviembre de 2022];23(10):1985-2004. Disponible en: <https://doi.org/10.1080/01431160110075532>
 11. Miller MD. The impacts of Atlanta's urban sprawl on forest cover and fragmentation. *Applied Geography* [Internet]. 1 de mayo de 2012 [citado 19 de noviembre de 2022];34:171-9. Disponible en: <https://www.sciencedirect.com/science/article/pii/S0143622811002335>
 12. Mirasi A, Mahmoudi A, Navid H, Valizadeh Kamran K, Asoodar MA. Evaluation of sum-NDVI values to estimate wheat grain yields using multi-temporal Landsat OLI data. *Geocarto International* [Internet]. 21 de julio de 2021 [citado 19 de noviembre de 2022];36(12):1309-24. Disponible en: <https://doi.org/10.1080/10106049.2019.1641561>
 13. Singla SK, Garg RD, Dubey OP. Sugarcane ratoon discrimination using LANDSAT NDVI temporal data. *Spat Inf Res* [Internet]. 1 de agosto de 2018 [citado 19 de noviembre de 2022];26(4):415-25. Disponible en: <https://doi.org/10.1007/s41324-018-0184-0>

14. Gil HAP, Ledezma EZ. Variations in vegetation cover using the normalized vegetation difference index to monitor SDGs in Manabí - Ecuador. *Revista Técnica de la Facultad de Ingeniería Universidad del Zulia* [Internet]. August 19, 2020 [cited 20 November 2022];(2):12-8. Available in: <https://produccioncientificaluz.org/index.php/tecnica/article/view/33610>
15. Ríos SJC, Zurita S, Rodríguez E, Montalvo V. Verification of NVI in rapieye images to determine vegetation cover and land uses in the province of Manabí, Ecuador. *San Gregorio Magazine* [Internet]. January 31, 2016 [cited November 19, 2022];2(10):75-92. Available in: <https://revista.sangregorio.edu.ec/index.php/REVISTASANGREGORIO/article/view/6>
16. PDOT. Plan de Desarrollo y Ordenación Territorial del Cantón Limón Indanza [Internet]. 2015. Available from: <https://multimedia.planificacion.gob.ec/PDOT/descargas.html>
17. Pimiento M. Multitemporal analysis of land use change in the paramo de pisba jurisdiction of the municipality of tasco for the period 1990 - 2015 [internet]. [Tunja]: UNIVERSIDAD PEDAGÓGICA Y TECNOLÓGICA DE COLOMBIA; 2019. Available in: <https://repositorio.uptc.edu.co/handle/001/3575>
18. Jensen JR, Lulla K. Introductory digital image processing: A remote sensing perspective. *Geocarto International* [Internet]. 1 March 1987 [cited 20 November 2022];2(1):65-65. Available in: <https://doi.org/10.1080/10106048709354084>
19. Ambrosio G, González J, Arévalo V. Radiometric and geometric correction of images for the detection of changes in a time series. 2012;9. Available in: <http://dspace.unach.edu.ec/bitstream/51000/4937/1/UNACH-EC-ING-AMBT-2018-0014.pdf>
20. Brizuela A, Aguirre C, Velasco I. Application of atmospheric correction methods of Landsat 5 data for multitemporal analysis. *Faculty of Agricultural Sciences UNER*. 2007;1(207-214).
21. Aguilar Arias H, Mora Zamora R, Vargas Bolaños C. Methodology for the atmospheric correction of Aster, Rapideye, Spot 2 and Landsat 8 images with the Flaash module of the Envi software. Atmospheric correction methodology for aster, rapideye, spot 2 and landsat 8 images with envi flaash module software. *REVGEO* [Internet]. May 1, 2015 [cited November 20, 2022];2(53):39-59. Available in: <http://www.revistas.una.ac.cr/index.php/geografica/article/view/6609>
22. International Telephone and Telegraph. Atmospheric Correction Module: QUAC and FLAASH User's Guide [Internet]. 2009. Disponible en: https://www.l3harrisgeospatial.com/portals/0/pdfs/envi/Flaash_Module.pdf
23. Isla R, Lopez R. Comparison of different vegetation indices for nitrogen deficiencies in maize. *XI National Congress of Remote Sensing*. 2005;24:93-6.
24. USGS. U.S. Geological Survey [Internet]. 2022. Disponible and: <https://earthexplorer.usgs.gov/>
25. Tovar CLM. The differential normalized index of vegetation as an indicator of forest degradation. *Unasylva: international journal of forestry and forest industries* [Internet]. 2011 [cited 21 November 2022];62(238):39-46. Available in: <https://dialnet.unirioja.es/servlet/articulo?codigo=3925443>
26. EOS DATA. NDVI: Frequently Asked Questions and What You Need to Know [Internet]. 2019. Available in: <https://eos.com/es/blog/ndvi-preguntas-frecuentes/>

27. Aguilar N, Galindo G, Fortanelli J, Contreras C. Normalized vegetation index in sugarcane in the Huasteca Potosina. *Advances in Agricultural Research* [Internet]. 2010 [cited 21 November 2022];14(2):49-65. Available in: <https://www.redalyc.org/articulo.oa?id=83715125003>
28. Rojas J. Estimation of the spatial and temporal variability of deforestation by alluvial gold mining in the Quebrada Guacamayo, using the method of segmentation by thresholds from satellite images [Internet]. [Lima]: Universidad Nacional Mayor de San Marcos; 2017 [cited 6 August 2022]. Available in: <https://library.co/document/zwk2dvvz-estimacion-variabilidad-deforestacion-quebrada-guacamayo-utilizando-segmentacion-imagenes.html>
29. USGS. Landsat Missions [Internet]. 2016. Available in: <https://landsat.usgs.gov/>.
30. Arango DF, Isabel M del PM, Hoyo LV del, Labrador JP. Estimation of the moisture content of vegetation from hyperspectral images acquired by the CASI (Compact Airborne Spectrographic Imager) sensor. *GeoFocus International Review of Geographical Information Science and Technology* [Internet]. 21 December 2015 [cited 21 November 2022];(16):177-204. Available in: <https://www.geofocus.org/index.php/geofocus/article/view/399>
31. Mejía V, Orellana D, Cabrera P. Land Use Change in the Northern Amazon of Ecuador: An Analysis Through VIIRS Night Satellite Imagery and LANDSAT Imagery. 2021;1:10-29. Available in: https://revistas.uazuay.edu.ec/html/revistas/UVERDAD/078/articulo01/uazuay.cambio_de_cobertura_de_suelo_en_la_amazonia_norte_del_ecuador.html
32. Chamba JA. Spatial and temporal dynamics of the Improved Vegetation Index (EVI) in the Ecosystems of southern Ecuador. [Internet] [bachelorThesis]. University of Azuay; 2015 [cited 7 December 2022]. Available in: <http://dspace.uazuay.edu.ec/handle/datos/4933>
33. Aldás AP. Analysis of the temporal dynamics of the normalized difference vegetation index (NDVI) for the years 1986, 2001 and 2017 in the Cotacachi Cayapas Ecological Reserve, Imbabura, through the use of google Earth Engine [Internet] [bachelorThesis]. PUCE-Quito; 2019 [cited 7 December 2022]. Available in: <http://repositorio.puce.edu.ec:80/handle/22000/16619>
34. Brito AM, Piedra BW, Altamirano D. Geological and geomorphological implications of the Upano river valley and the bridge of the Macas – Puyo road, Morona Santiago, Ecuador [Internet] [Thesis]. 2021 [cited 7 December 2022]. Available in: <http://www.dspace.espol.edu.ec/handle/123456789/52328>